CNRS
Centre National de la Recherche Scientifique

INFN
Istituto Nazionale di Fisica Nucleare

Auxiliary Laser system: study of the lock acquisition strategy

VIR-0327A-19

Julia Casanueva[2*] and Nicolas Leroy[1]

[2] *INFN - Sezione di Pisa*
[1] *LAL - Laboratoire de l'Accelerateur Lineaire*

Date: April 2, 2019

[*] *corresponding author:* julia.casanueva@pi.infn.it

VIRGO* A joint CNRS-INFN Project
Via E. Amaldi, I-56021 S. Stefano a Macerata - Cascina (Pisa)
Secretariat: Telephone (39) 050 752 521 * FAX (39) 050 752 550 * Email: ego@ego-gw.it

Contents

1 Introduction

One of the upgrades planned in order to improve the sensitivity is the addition of a new optical cavity to recycle the signal coming from the passage of a Gravitational Wave (GW). It has already been installed at LIGO detectors, improving the sensitivity at high frequency (above $\sim$ 200 Hz) without affecting the performance at low frequency [1]. However, the new Signal Recycling Cavity (SRC) adds an extra longitudinal Degree of Freedom to be controlled, which makes more complex to bring the interferometer to its working point.

The LIGO collaboration had to come up with a new control strategy to deal with the SRC, which was based on the use of Auxiliary Lasers. This document presents a careful study of this control strategy and proposes the modifications needed to adapt it to the Advanced Virgo detector, taking also in account the fibered auxiliary laser source proposed in the Virgo note [2]. As this strategy has already been succesfully applied in LIGO, we will focus on the differences with Virgo, and thus on the points which might need modifications. The simulations have been made using finesse [3] and supposing an input power of 25 W, which implies a reflectivity of the Signal Recycling mirror of R = 0.5.

2 Control acquisition strategy

As mentioned in the introduction, the addition of a new optical cavity implies one more length to control so that it is kept on resonance, the Signal Recycling Cavity Length (SRCL). In this optical configuration there are 5 longitudinal Degrees of Freedom (DOFs) in total, which are shown in Figure 3.

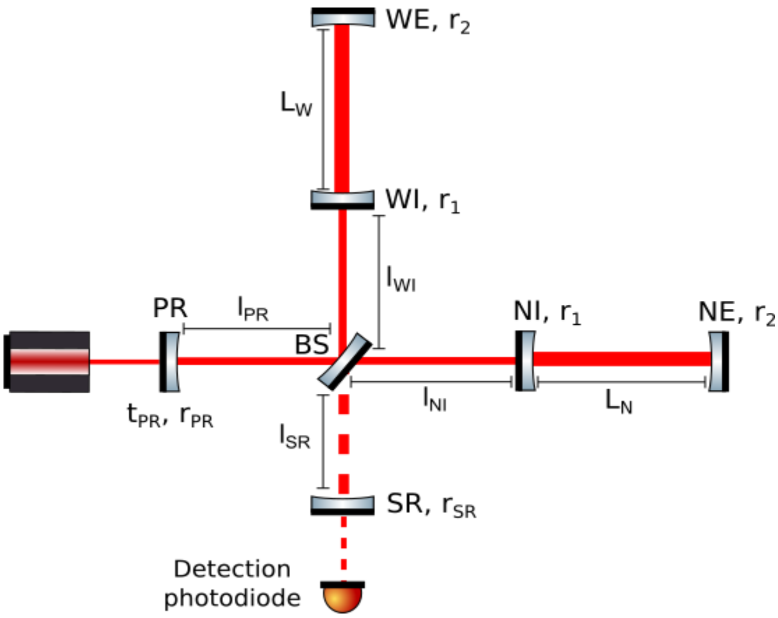

Figure 1: Optical configuration of Advanced Virgo. All the relevant lengths are indicated.

The desired working point of the interferometer in this configuration is to have both arm Fabry-Perot cavities on resonance, as well as the Power Recycling Cavity (PRC) and the SRC. The Michelson interferometer (MICH) is expected to be on its Dark Fringe. The different longitudinal DOFs can be defined as:

$$\begin{aligned} DARM &= \frac{L_N - L_W}{2} \\ CARM &= \frac{L_N + L_W}{2} \\ MICH &= l_{NI} - l_{WI} \\ PRCL &= l_{PR} + \frac{l_{NI} + l_{WI}}{2} \\ SRCL &= l_{SR} + \frac{l_{NI} + l_{WI}}{2} \end{aligned} \tag{2.1}$$

It is important to notice that the arm cavities can not be controlled independently but in terms of its Common length (CARM) and its differential length (DARM). This is because GWs are expected to produce a differential change on the length of the arms, which will be seen by the DARM DOF.

Moreover, it is also convenient to work in terms of Common DOF, since it is the only DOF which has two contributions: the length noise, coming from the movement of the mirrors due to the seismic noise; and the frequency noise, coming from the laser source. Even is there is a pre-stabilization of the frequency noise, based on the Reference Cavity (RFC) at low frequency and the Input Mode Cleaner (IMC) at higher frequencies, it is the dominant noise on all the sensors of the interferometer. This makes the control of the Common DOF one of the key parts of the lock acquisition strategy.

However, it is not possible to engage the control of all the 5 DOFs simultaneously, since the mirrors move in a random way and the working point is rarely crossed spontaneously. For this reason a control strategy is needed. Initially at LIGO, the control strategy consisted in engaging simultaneously the control of the two central DOFs on the sideband resonance and then engaging the arms control. However, this scheme could not be used anymore for the Advanced LIGO detector, since the addition of the SRC increases strongly the coupling of the longitudinal DOFs.

Instead, the Virgo interferometer designed a different control strategy, since the suspensions would get easily excited during the transients of the previously described process. The Variable Finesse strategy consisted in acquiring the control of the interferometer in an intermediate state first, with the PR mirror misaligned. This fact is very important because it makes one DOF ”disappear”, and reduces the coupling between the remaining four. Moreover, the Michelson DOF is acquired in Half-Fringe, far from its target working point, where the finesse of the overall interferometer is lower than the nominal one, which simplifies further the task. Once all the DOFs are under control, the interferometer is brought to its nominal working point passing through stable intermediate states and avoiding transients.

The presence of the Signal Recycling Mirror between the asymmetric port and the BS makes very difficult the application of the Variable Finesse strategy, since it partially reflects the light back to the interferometer. Moreover, due to the optimization of the LIGO mirror actuators, the dynamics available was not enough to engage the control of the arm cavities, so another strategy was developed to lock Advanced LIGO based on the use of Auxiliary Lasers.

2.1 Lock with Auxiliary Lasers

The basic principle is the same as for Variable Finesse: reduce the DOFs to be controlled initially and acquire the control of the whole interferometer (all the DOFs) in an easier intermediate configuration. So the first step is to eliminate two DOFs, the arm cavities (CARM / DARM), keeping them out of resonance. For this purpose, two green Auxiliary Lasers are placed at the end benches, entering the interferometer through the end mirrors.

There are several advantages of using these Auxiliary Lasers. In the first place, we can lock the laser to the cavities, which eliminates the control transients that can not be handled by the new mirror's actuation.

Moreover, the coating of the mirrors has been chosen so that the finesse seen by the green lasers is smaller than for the infrared (IR). This also eases the acquisition of the control of the arms. Finally, by adding an offset with respect to the main laser, the arm cavities can be kept under control (on resonance for the Auxiliary Lasers) but outside the resonance of the main laser.

Once the arms are "invisible", the 3 remaining DOFs of the Central Interferometer (CITF) are controlled. The control is engaged first using the nominal error signals, and then it is handed-off to the 3f error signals. This part is key on the control strategy since these error signals are weakly sensitive to CARM DOF. Thanks to them, the central DOFs will be decoupled from the arm cavities ones while they are brought to their working point.

At this point all the DOFs are under control but they do not interact due to the frequency offset or CARM offset between the main laser and the auxiliary ones. Slowly, this offset is reduced and the arms are brought to the IR resonance, so the final working point.

3 First step: control of the arm cavities

In this section we are going to analyse in detail the Advanced LIGO control strategy for the arms, until the offset is added between the main and the auxiliary lasers, and how to adapt it to Virgo.

The Auxiliary Lasers are injected into the interferometer from the terminal benches, that is, through the end mirrors. Then, they need to be locked to the main laser if we want to keep the arm cavities far from the resonance of the IR. In Advanced LIGO, the green lasers used as Auxiliary Lasers are two different laser sources, one on each terminal bench, locked in phase to the main laser via a PLL (Phase Locked Loop). For Advanced Virgo instead, there has been a proposal [2] to bring two peak-offs of the main beam to the end benches and double them to obtain the two green laser beams. This way, there is no need for a PLL, since the Auxiliary Lasers are directly related to the main one.

In both cases, the peak-offs of the main laser are brought to the end benches using 3km of optic fiber. This introduces extra phase noise to the beam arriving to the end benches, and so the Auxiliary Lasers are expected to be noisier than the main laser beam.

3.1 Auxiliary Lasers to arm cavities loop

The first step of the control strategy is to lock the arm cavities to the Auxiliary Lasers. This way, the arm cavities are kept on resonance for the green laser, offering at the same time a good pre-stabilization of the green laser frequency noise. It is worth mentioning that in the LIGO case, the finesse of the arm cavities is lower (less than 10 for Hanford and several tenths for Livingston) than in Virgo, which is approximately 150. Due to the higher finesse, the Virgo cavities will be a better reference, and so the frequency noise reduction will be higher.

On the other hand, the control acquisition will be more affected by the initial amount of phase noise (either from the seismic noise or from the passage through the optical fiber). For this reason, a measurement of the phase noise expected after the passage through 3km of optic fiber has been made in [4]. Using this information, simulations were made in order to confirm that with the expected phase noise (both seismic and fiber noise components), a loop with an UGF of 10kHz would be enough to engage the control of the Virgo arm cavities [4].

LIGO control scheme proposes to build up an error signal for this loop in reflection of the arm cavities (at the terminal benches, since the Laser Aux enter the cavities through the end mirrors), using a classic PDH technique. The scheme proposed at Virgo, follows this idea but proposes to use the Acousto Optical Modulator (AOM) in order to modulate in phase the beam ($\sim$ 35 kHz) and build the error signal. This would have the advantage of avoiding the installation of an extra element (an Electro Optical Modulator), re-using instead the AOM that is already used for the power stabilization and the addition of the CARM frequency offset.

Finally, at LIGO, the actuation is split between the end mirror of the cavity at low frequencies (up to 100 Hz) and the green laser frequency itself, via the PLL, at high frequencies (up to 10kHz). This is done because at low frequencies, where the seismic noise is more relevant, the mirror's actuators have a wider dynamic range. In Virgo, the corrections at high frequencies will be applied to the AOM instead.

Once these loops are closed (one for the north arm and another for the west one), the green lasers are transmitted by the arm cavities, now stabilized in frequency to better than the linewidth of the cavities ($\sim$ 300 Hz). At this point, the main target is fulfilled: the arm cavities are under control using the Laser Aux, which have a known relationship with the main laser.

3.2 Main laser frequency stabilization

In the previous step, we have reduced the Auxiliary Lasers frequency noise, and the cavities' length fluctuations due to the seismic noise. However, the frequency noise from the main laser is still at its pre-stabilization stage, which uses the Reference Cavity (at low frequency) and the Input Mode Cleaner (at high frequency) as references. This control does not suppress the main laser frequency noise enough to engage the control of the interferometer. For this reason, once the arm cavities are under control, we use them at low frequency, instead of the IMC, since they are the best reference available. This control is also known as Second Stage of Frequency Stabilization in Virgo.

In order to build-up the error signal, LIGO proposes to use the transmitted green laser beam as reference, and make it interfere with the main laser beam (doubled). For this purpose they shift the frequency of the beam that is sent to the end benches, and in consequence the frequency of the Auxiliary Lasers, by f_{arm}, using an AOM. Initially the detection scheme was the following: one error signal was extracted from the beating between north and west arm (DARM) and the other one from the beating between one arm and the main laser (CARM). However, this scheme was not exact, since the CARM error signal was only correct if the DARM loop was closed. To avoid this coupling, and to minimize the sensing noise, the detection scheme was updated [5].

Nowadays, the error signal is extracted from the beating of each of the arms separately with a peak-off of the main laser beam, after being doubled. Demodulating at f_{arm} ($\sim$80 MHz), we can get the information concerning the phase difference between the main laser and each of the cavity lengths. In principle we get two error signals, one from the North arm and another from the West one, that need to be combined to build up the Common (the sum of both error signals) and Differential (the difference between both error signals) DOFs. We propose to follow this same scheme, which seems to be more precise.

A this point, the CARM error signal is used as a substitute of the RFC one, to control the IMC. At higher frequency the CARM error signal is used to control the laser frequency. In the case of Virgo, the nominal UGF of this part of the loop is around 15 kHz, even if during the lock acquisition it is much lower (1-5 kHz). Nevertheless, the UGF of this second loop will depend of the interferometer needs and on the quality of the error signal, that is, the sensing noise. For LIGO, an UGF of 200 Hz is enough during the lock acquisition, which implies that only the first loop is necessary (the IMC one). Notice that in Virgo the linewidth is 3 times lower, so our SNR will be higher, and we could improve the bandwidth if needed. Regarding the DARM error signal, it is filtered and sent to the end mirrors, together with the correction from the Auxiliary Lasers loop.

3.3 CARM offset

The last step is to add an offset between the Auxiliary Lasers and the Main laser to avoid the last one to resonate inside the arm cavities. The idea is to keep the DARM loop closed, while putting an offset to the CARM DOF, that would bring the main laser out of the resonance.

In the LIGO case, this offset is added to the main laser by tuning the IMC length. In principle, due to the PLL that locks the Auxiliary Lasers to the main laser, this offset would be ineffective, and the green lasers would follow the main one. However, the corrections of the Auxiliary Lasers loop to the arm cavities are sent to the PLL as well, overriding any offset coming from the main laser.

In Virgo, the offset can not be added to the IMC, since the Auxiliary Lasers are a peak-off of the main one, doubled. Instead, it will be necessary to add an offset both to the AOMs that are used for shifting the Auxiliary Laser frequency and to the PLL in transmission to avoid the main laser to follow. The idea is to make a scan of the main laser resonance by changing the offset added to the AOM, and then fix the offset at a value where it is non-resonant.

At this point we have both the main laser and the Auxiliary Lasers stabilized in frequency, and the Differential DOF also under control. Finally, thanks to the offset, the Auxiliary Lasers are kept resonant on the cavities, while the main laser is not. Now there are two degreed of freedom controlled, but not interfering with the other three, and so we can pass to acquire the control of the Central Interferometer (CITF).

4 Second step: control of the Central Interferometer

Once the arm cavities are controlled, we can pass to the central degrees of freedom: MICH, PRCL and SRCL. In order to choose the best error signals it is necessary to take in account the next step in the lock strategy, the CARM offset reduction. This implies that its frequency response will change for every offset, and so will do the one of the rest of longitudinal DOFs. In particular the carrier passes from anti-resonant to resonant in the arms which implies a phase change of 180° of the reflected field. Moreover, CARM is the most critical DOF due to its contribution from the laser frequency noise, which makes it couple strongly to all the photodiodes (and in consequence to all the error signals) available.

For this reason in LIGO are using the *3f* error signals, since they depend weakly on the carrier and strongly on the sidebands, which are resonant on the Central Interferometer and not on the arm cavities. This have several advantages among which, the one that interests us, the insensitivity to the CARM DOF [6]. The disadvantage of this error signals is that they have a low SNR. However, during the lock acquisition the priority is the robustness and not the sensitivity so the idea is to use them during the CARM offset reduction, and hand them off to the optimal f error signals once in the final working point.

In LIGO, due to the low SNR of the *3f* error signals, the final ones (f) are used for the lock acquisition, since at the beginning the interferometer is in a temporary steady state. Once the CITF is under control, the error signals are handed-off to the *3f* ones before starting the offset reduction.

4.1 Working point and f error signals

Before studying the best error signals, it is necessary to define the working point. For MICH and PRCL the conditions are the same as for the PRITF: destructive interference at the detection port and carrier resonant on the PRC. To build up the different error signals two modulation frequencies were added: f_1 = 6 MHz and f_2 = 8 MHz. f_1 is the modulation used to control the arm cavities. For this reason it was chosen to be resonant on the PRC but anti-resonant on the arm cavities. f_2 instead was chosen to control the PRC and for this reason it is anti-resonant on the PRC, so it does not enter into the ITF.

Regarding the SRC, its role is to recycle the signals produced by the passage of gravitational waves. They appear as sidebands around the carrier, which leak to the anti-symetric port. Several working points of the SRC have been considered since the frequency bands where the sensitivity is improved will change accordingly. However, to simplify the control of this cavity the simplest configuration is to work on anti-resonance of the carrier. In order to create a good error signal, a new modulation frequency has been added, f_3 = 6 MHz * 9 = 56 MHz. It is the lowest modulation frequency which is an odd multiple of the 6 MHz (the even multiples are not resonant on the PRC) and which resonates on the SRC [7]. So in practice the carrier acts as a phase reference, since it is anti-resonant, while the 56MHz enters into the cavity providing information about its length. The plan is then to lock the SRC on the 56MHz. This information is summarized on Figure 2.

As it was mentioned on the introduction, the idea is to acquire the control of the three central dofs using f_1 error signals since their SNR is better. The proposal from LIGO is to use B2 6MHz to control PRCL (see Figure 3),

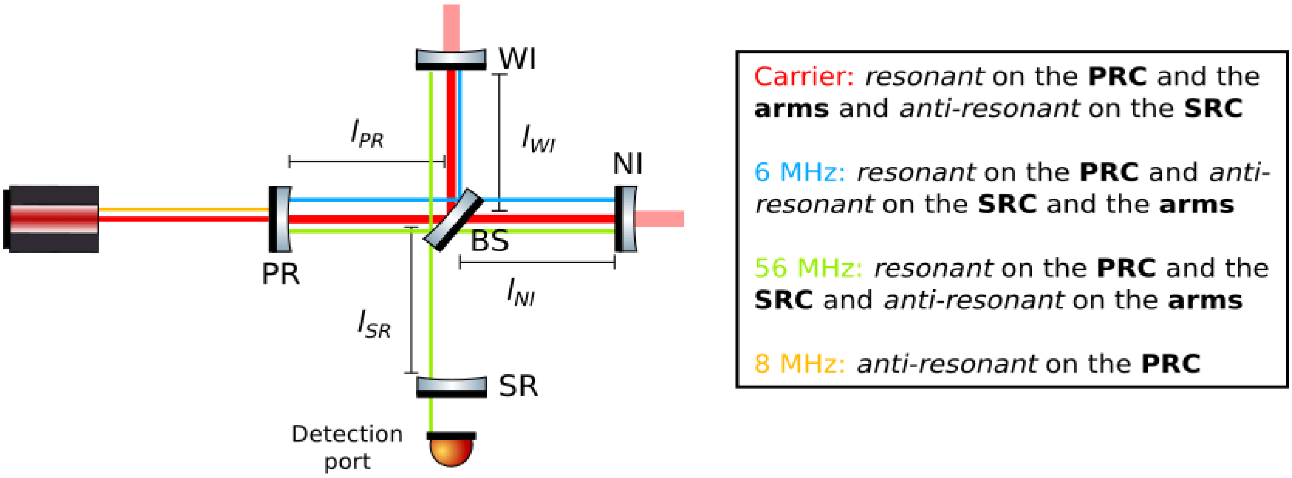

Figure 2: Optical scheme of the Advanced Virgo interferometer with the Signal Recycling Mirror (SR).

since they do not have a modulation frequency anti-resonant on the PRC. For us both of them are suitable.

Regarding SRCL and MICH dofs, the proposal was to use both quadratures of B2 56 MHz. From the compass plot in the middle of Figure 3 it can be seen that both dofs are well decoupled, since they are 90° away. However, PRCL and SRCL are completely coupled. For this reason it might be necessary to combine two error signals to diagonalize the sensing matrix. It is enough to substract the error signal used for PRCL to the SRCL one.

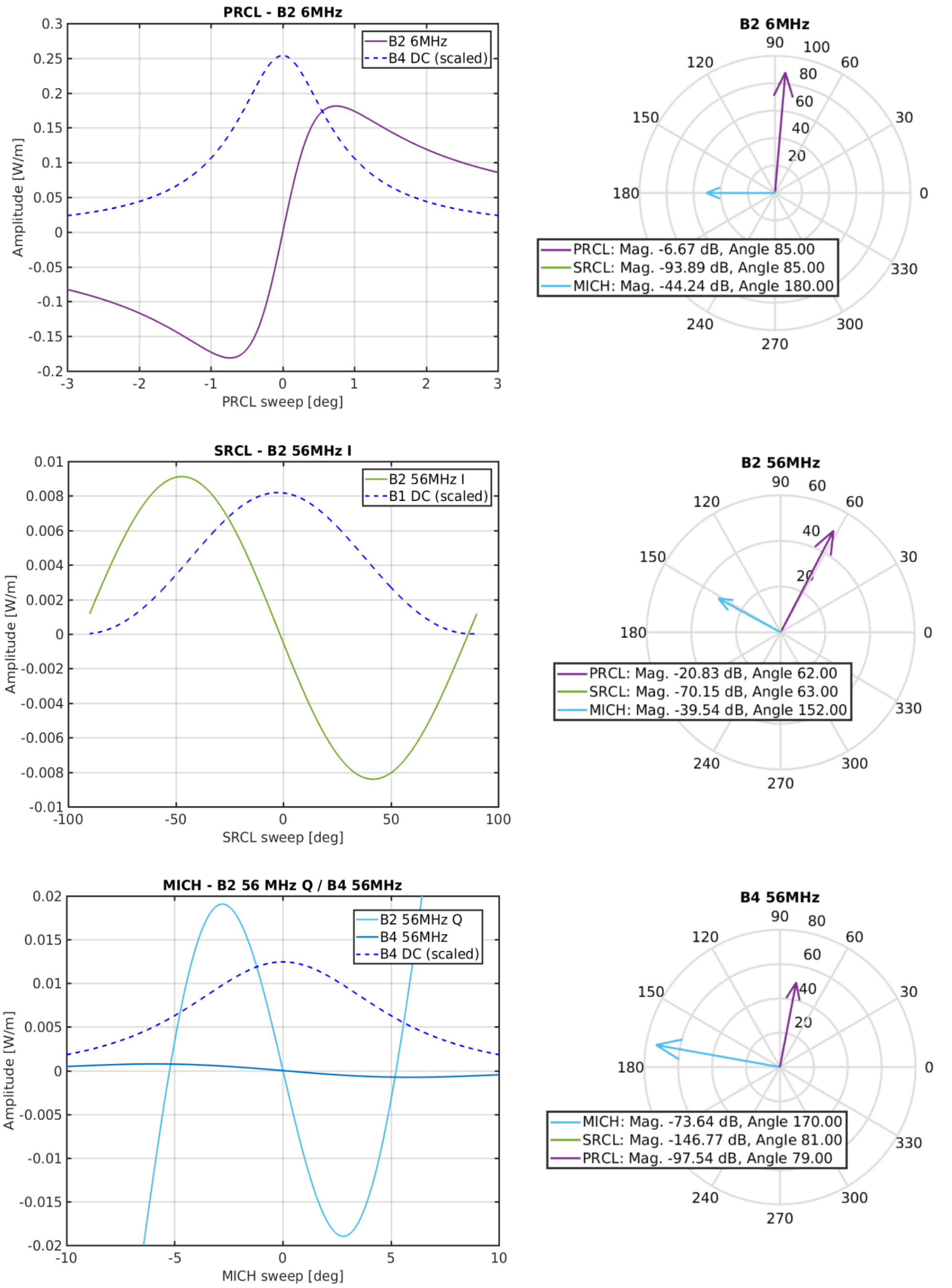

Figure 3: Error signals of the central interferometer degrees of freedom, compared to their resonance peaks (dashed lines) on the left. The right figures show the coupling between these degrees of freedom for each of the error signals. The maximum optical gain that can be achieved for each degree of freedom and the corresponding demodulation phase are plotted for this purpose. **Top plot:** PRCL error signal, B2 6 MHz. *Central plot:* SRCL error signal, B2 56 MHz I. **Bottom plot:** MICH error signals, B2 56 MHz and B4 56 MHz.

Finally, the bottom plot on Figure 3 shows a scan of the MICH dof. B2 56MHz Q has a very hogh optical gain but it has several zero-crossings. In case this becomes a problem, in the same plot it can be seen B4 56MHz, which has a lower optical gain but only one zero crossing.

Regarding the lock acquisition of these degrees of freedom, the technique used is described in [8].

4.2 Choice of *3f* error signals

Once the central dofs are controlled, it is necessary to replace the error signals by the 3f ones, which are insensitive to the reduction of the CARM offset. We have studied the 3f error signals at different CARM offsets to check their linearity and whether they suffer important changes. In Figure 4 it can be seen that the error signals barely change with the CARM offset, keeping their linearity during all the process.

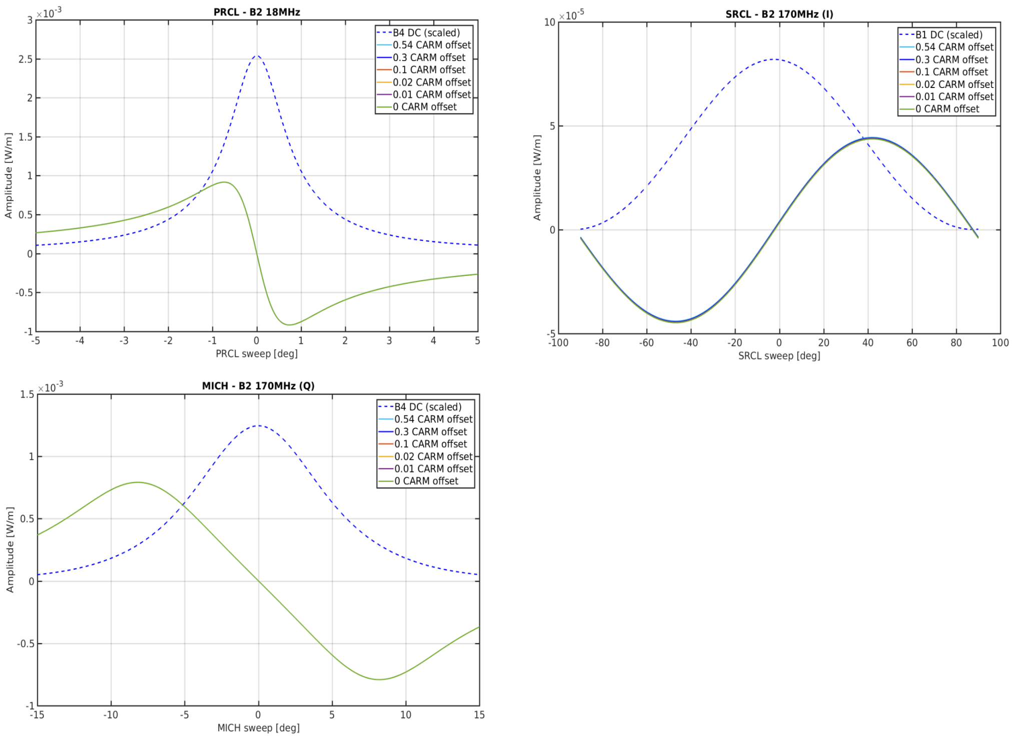

Figure 4: *3f* error signals for controlling the central degrees of freedom during CARM offset reduction (in degrees). **Top-right plot:** PRCL error signal, B2 18 MHz. **Top-left plot:** SRCL error signal, B2 170 MHz Q. **Bottom-right plot:** MICH error signal, B2 170 MHz Q

The challenge of this part in Virgo is that we need the *3f* of the second modulation frequency, which corresponds to ∼168MHz. This is not within the nominal detection bandwidth of the photodetectors, but they are not completely insensitive. As they are only used during lock acquisition a high SNR is not needed, but we need robust signals instead.

5 Final step: hand-off of DARM / CARM

The last step of the lock acqusition is to stop controlling CARM and DARM with the Green Laser signals and to start using IR signals until reaching the working point with the nominal error signals. During the CARM offset reduction the error signals coming from the IR beam change strongly, as the optical configuration also changes. Figure 5 shows how the power of the main laser on the different photodiodes changes during the CARM offset reduction.

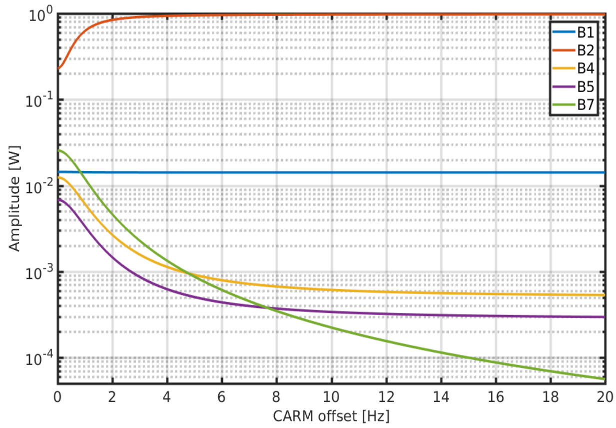

Figure 5: Power reaching the main photodiodes during the lock acquisition.

For this reason it is necessary to check when the IR signals start to make sense, and when we can start using them. This analysis showed very similar results as the simulations done by LIGO [9].

5.1 PDH error signals

The first step is to check when the error signals we want to use in the steady state start to be linear: B2 6MHz for CARM and B1p 56MHz for DARM. For this purpose we have checked the transfer function between the dof and the error signal for different CARM offsets. The results are shown in Figures 6 and 7.

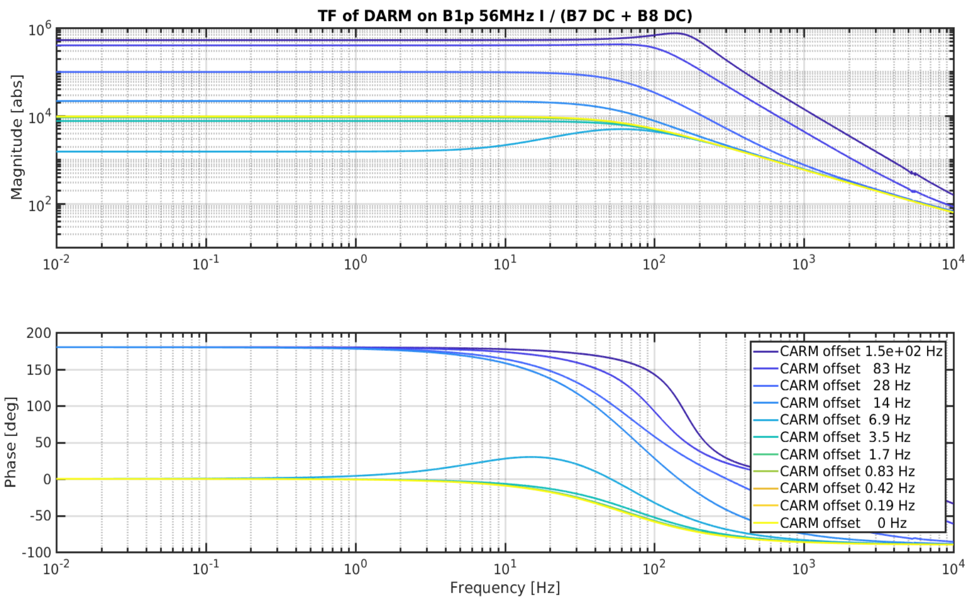

Figure 6: Transfer function between B1p 56 MHz and DARM for different CARM offsets.

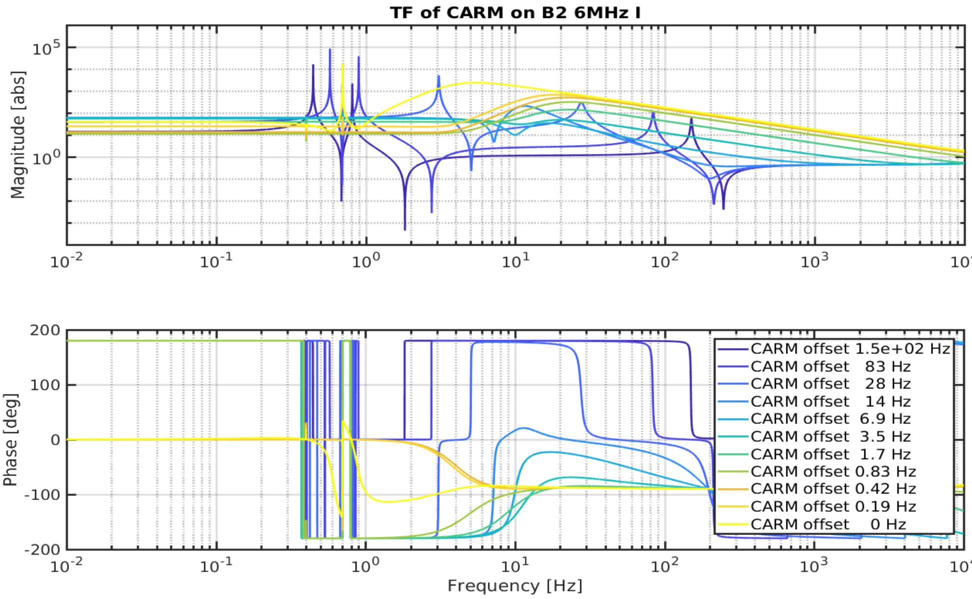

Figure 7: Transfer function between B2 6 MHz and CARM for different CARM offsets.

The shape of the transfer function of the error signal of DARM, B1p 56MHz, remains quite constant over the CARM offset reduction, as shown in Figure 6. However, the phase shows a change of sign when we get far from the resonance (CARM offset 0Hz). According to the simulation, the final DARM error signal can be used already at 7 Hz of CARM offset. Also notice that starting from 3.5 Hz of CARM offset, the optical gain remains unchanged.

Regarding CARM error signal, radiation pressure effects has been taken in account in the simulation, since the cavity is detuned due to the offset. According to Figure 7 this error signal can be used starting only from 0.5 Hz, since at higher offsets the phase is wrong by 180°.

We have also studied the possibility to normalize these error signals in order to further increase their linear region. Figure 8 shows a comparison between the error signal of CARM and DARM with and without normalization. In both cases the linear region is increased, in the case of CARM up to ∼40 Hz and for DARM up to ∼20 Hz. So using the transmitted power of the cavities to normalize the PDH signals will be also helpful to simplify the CARM offset reduction process.

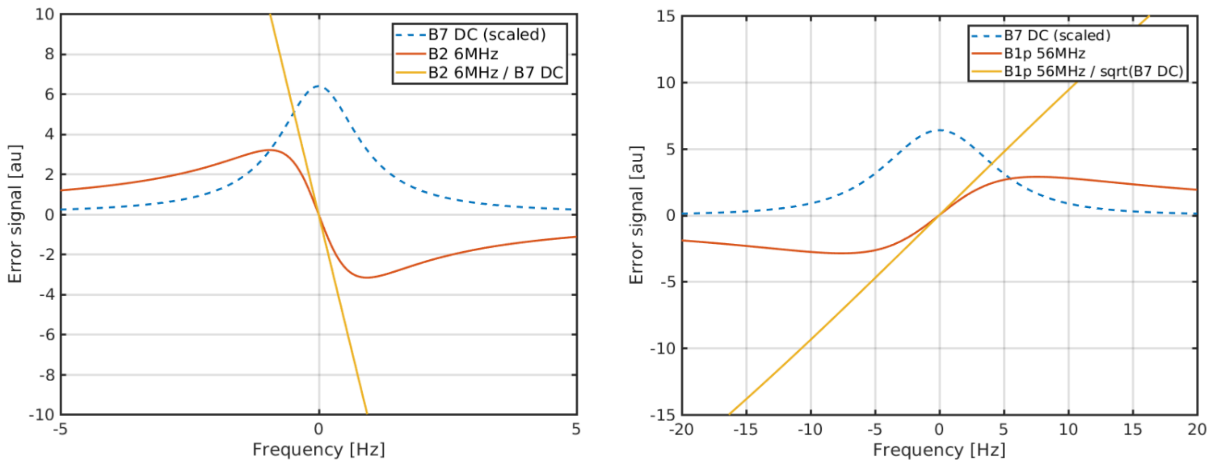

Figure 8: **Left plot:** CARM error signal, B2 6 MHz, with and without normalization (yellow and red curves respectively) compared to the resonance width of the arm cavities. **Right plot:** DARM error signal, B1p 56 MHz,with and without normalization (yellow and red curves respectively) compared to the resonance width of the arm cavities.

5.2 Transition error signals

Once we know when we can start using the nominal error signals, we need to look for error signals to use in the meantime if necessary. This choice is mainly influenced by the CARM loop precision that can be achieved using green laser signals only. In the LIGO case, they manage to control it as to get 30 Hz of rms. They stop using green laser signals once the CARM offset is so small that the residual movement of the CARM loop might cause an accidental crossing of the resonance ($\sim$15 Hz).

In the case of Virgo the finesse of the arm cavities for the green laser is $\sim$10 times higher than in LIGO. If we take in account the difference of Free Spectral Range, implies that we have 3 times more of optical gain on the green signals. So we expect to be able to get closer to the resonance before being obliged to change to IR signals.

In the case of DARM, the PDH signal is already linear at 7 Hz, so we could try to make the passage from green to the nominal error signal directly, without the need of any intermediate error signal. The proposal is then to decrease the CARM offset down to 7 Hz while using the green signals, and make at this point the first hand-off for CARM/DARM.

At this step there is already $\sim$2% of the maximum IR power transitted by the arms, so we can use the photodiodes in transmission as error signals to improve the CARM loop precision and so the stability of the transmitted power itself before handing-off DARM to an IR error signal. Figure 9 shows the transfer function between CARM and (B7 DC + B8 DC) for different CARM offsets.

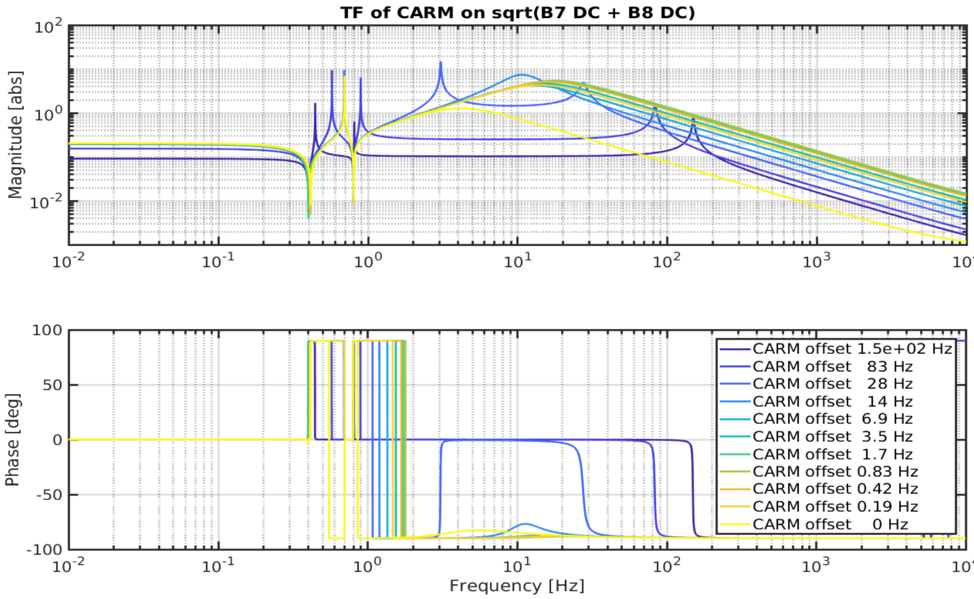

Figure 9: Transfer function between sqrt(B7 DC + B8 DC) and CARM for different CARM offsets.

Regarding the phase, it is constant for all the CARM offsets, however, there are several structures due to the detuning of the cavity and radiation pressure that changes strongly during this process. Starting from 7 Hz the peak due to the detuning of the cavity stabilizes its frequency (∼25 Hz) and its quality factor, so the TF shape becomes more stable. LIGO proposes a blending with the green signals: use the IR under 30 Hz to improve the precision, but the green up to 300 Hz if necessary.

If this improvement on the CARM loop does not increase the stability of the arm cavities to use B1p 56 MHz for DARM, we have also studied the possibility of using the transmitted power, as for CARM. The TFs are shown in Figure 10. Also in this case the phase is the good one for all offsets, but as there is no detuning in this case, the TF shape is much more stable.

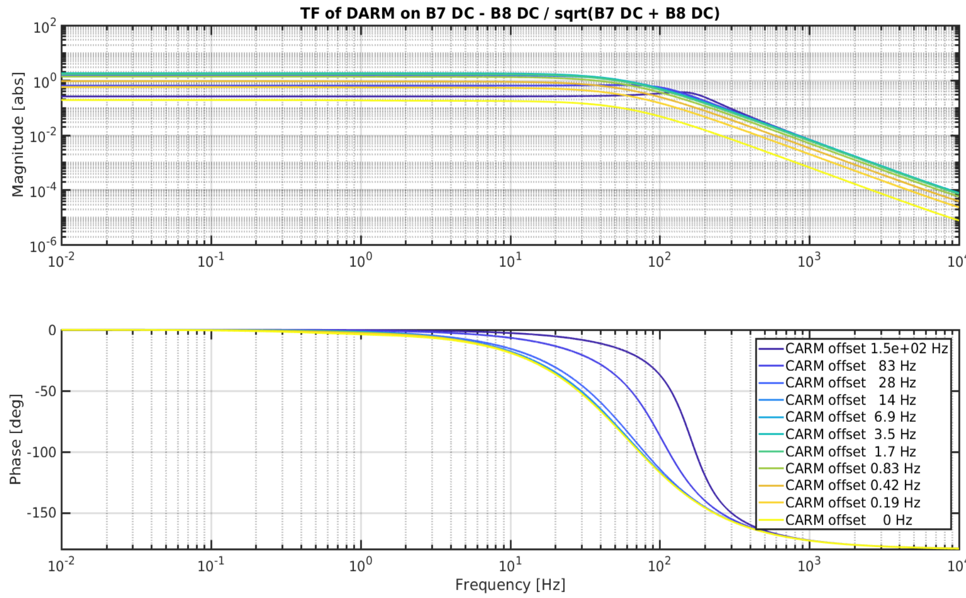

Figure 10: Transfer function between (B7 DC - B8 DC/sqrt(B7 DC + B8 DC)) and DARM for different CARM offsets.

After this first hand-off, hopefully we will control DARM already with the final signal, but CARM is still on a temporary error signal. For the final transition, LIGO chose its error signals based on the strong coupling of CARM to the SRCL error signal while very close to the resonance (9 nm @ ∼2 Hz). We have checked this coupling for Virgo, as shown in Figure 11, and it does not present the same behaviour as in LIGO. It is higher when far from resonance (∼4 nm @ 50 Hz) and it decreases while getting closer to resonance (<0.2nm @ 2 Hz). So this coupling will not be a problem in our case (our SRC has a finesse of ∼4 while in LIGO it is ∼14), and we will not be forced to pass to a IR-signal in the whole bandwidth at 2 Hz, until we can make the hand-off to the PDH signal, or until the precision of CARM will not be enough.

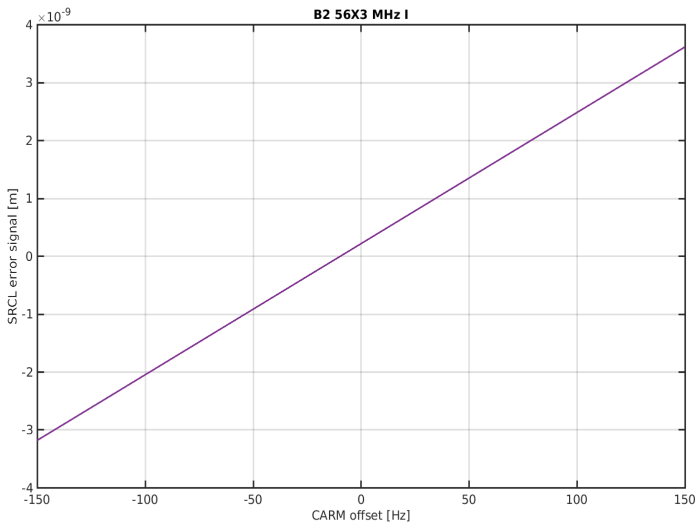

Figure 11: Error signal of the SRC (B2 56x3 MHz) while sweeping CARM, calibrated in meters.

DOF	Error signal
DARM	B1 DC
MICH	B4 56 MHz I
SRCL	B4 56 MHz Q
CARM	B2 6 MHz
PRCL	B2 8 MHz

Table 1: Proposal set of error signals to be used at the final working point. Notice that if needed PRCL error signal could be used to decrease the coupling to SRCL by subtracting it.

After putting the CARM offset to 0 it is the moment to hand-off the error signals of the central interferometer to the nominal *1f* error signals shown in 1.

6 Conclusion and perspectives

We have analyzed the lock acquisition used at LIGO, focusing on the differences between our optical designs. The simulations do not show any unexpected problem, so apart from the experimental challenges (use of 56x3 MHz, use of 6 MHz) the strategy should work also for Advanced Virgo.

For this work we have had many exchanges with Kiwamu Izumi, who has work on this system for LIGO and now for KAGRA. These exchanges continue, since the auxiliary lasers technique has been modified for KAGRA, in an optical design which could decrease significantly the hardware complexity as well as the cost. This option will be explored in the next future, even if from the lock acquisition point of view the changes would be minimal, the major impact would be in the green laser signal generations.

References

[1] H. Heitmann, 'O3 preparation', Virgo Presentation, 2017, VIR-0348A-17. 2

[2] A.Chiummo, E.Genin, N.Leroy, A.Magazzu, M.Mantovani, F.Paoletti, G.Pillant, 'All Fibered 532nm laser source for AdV Auxiliary Lasers', Virgo note, 2016, VIR-0542A-16 2, 4

[3] A. Freise, G. Heinzel, H. Luck, R. Schilling, B. Willke and K. Danzmann, 'Frequency domain interferometer simulation with higher-order spatial modes', Class. Quant. Grav. 21 (2004) S1067 [arXiv:gr-qc/0309012]. 2

[4] J. Casanueva, G. Pillant, E. Genin, N. Leroy, 'Auxiliary Laser system: fibre phase noise measurement and cavity lock requirements', Virgo note, 2016, VIR-0540A-16 4

[5] K. Izumi, 'Notes on the coupling issue in aLIGO Arm Length Stabilisation', LIGO note, 2013, LIGO-T1300923-v1 5

[6] K. Arai, M. Ando, S. Moriwaki, K. Kawabe, K. Tsubono, 'New signal extraction scheme with harmonic demodulation for power-recycled Fabry-Perot-Michelson interferometers', Physics Letters A 273 (2000) 6

[7] G. Vajente, R. Day, J. Marque, 'AdV optical layout: new parameters proposal', Presentation, 2011, VIR-0377B-11 6

[8] D. Martynov, 'Lock Acquisition and Sensitivity Analysis of Advanced LIGO Interferometers', PhD, California Institute of Technology, Pasadena (2015) 9

[9] K. Izumi, S. Dwyer, L. Barsotti, 'Simulation Study for aLIGO Lock Acquisition', LIGO note, LIGO-T1400298-v1 10